

**CRACK DETECTION OF EGGSHELL  
FEATURING AN IMPROVED ANISOTROPIC  
DIFFUSION FILTER AND SUPPORT VECTOR  
MACHINE**

**MOHD HAFIDZ B. ABDULLAH**

**UNIVERSITI SAINS MALAYSIA**

**2018**

**CRACK DETECTION OF EGGSHELL FEATURING AN IMPROVED  
ANISOTROPIC DIFFUSION FILTER AND SUPPORT VECTOR MACHINE**

**by**

**MOHD HAFIDZ B. ABDULLAH**

**Thesis submitted in fulfillment of the  
requirement for the degree of  
Doctor of Philosophy**

**June 2018**

## **ACKNOWLEDGMENT**

First and foremost, I would like to express my gratitude to my supervisor Prof. Dr. Mohd Zaid B. Abdullah for the guidance, useful comments and discussions, and the most for the encouragement given to me during my study. Also, my deepest thanks to the Universiti Kuala Lumpur (UniKL) and Universiti Sains Malaysia (USM) for the scholarship and resources provided to me in the whole 4 years of study. Furthermore, I would like to thank my colleagues and friend who always support and encourage me. Finally, thanks to my family especially to my parents for the continuous support, prayer and always be by my side to courage me for the completion of this study.

## TABLE OF CONTENTS

	Page
<b>ACKNOWLEDGEMENT</b>	ii
<b>TABLE OF CONTENTS</b>	iii
<b>LIST OF TABLES</b>	vi
<b>LIST OF FIGURES</b>	vii
<b>LIST OF ABBREVIATIONS</b>	x
<b>LIST OF SYMBOLS</b>	xii
<b>ABSTRAK</b>	xiv
<b>ABSTRACT</b>	xvi
<b>CHAPTER ONE: INTRODUCTION</b>	
1.1 Introduction	1
1.2 Crack Inspection	1
1.3 Research Problems	4
1.4 Research Objectives	7
1.5 Research Scope	8
1.6 Thesis Organization	8
<b>CHAPTER TWO: LITERATURE REVIEW</b>	
2.1 Introduction	9
2.2 Image Processing	9
2.3 Anisotropic Diffusion Filter	10
2.4 Segmentation	23
2.5 Pattern Representation	30
2.5.1 The Implementation of Radon Transform	37
2.6 Machine Learning	39

2.6.1	Twin Bounded Support Vector Machine	40
2.6.2	The Implementation of Twin Bounded Support Vector Machine	42
2.6.3	Multi-class Classification	44
2.6.3(a)	One-versus-all (OVA)	45
2.6.3(b)	One-versus-one (OVO)	45
2.6.3(c)	Directed Acyclic Graph (DAG)	46
2.7	Crack Detection Techniques	47
2.8	Summary	54

### **CHAPTER THREE: METHODOLOGY**

3.1	Introduction	57
3.2	Line Enhancement	57
3.3	Crack Analysis	58
3.4	Anisotropic Diffusion Filter	60
3.5	Double Thresholding	67
3.6	Crack Detection System	71
3.6.1	Research Methodology	72
3.6.2	Imaging Set-up	72
3.6.3	Egg Sample	74
3.6.4	Image Preprocessing and Segmentation	76
3.6.5	Feature Extraction and Reduction	79
3.6.6	Classification	81
3.6.7	Performance Evaluation	82
3.7	Summary of Crack Detection System	87

### **CHAPTER FOUR: RESULTS AND DISCUSSION**

4.1	Introduction	89
4.2	Image Processing	89
4.2.1	RGB Image Decomposition	90
4.2.2	Background Estimation	93

4.2.3	Line Enhancement	94
4.2.4	Anisotropic Diffusion Filtering	96
4.3	Image Segmentation	101
4.4	Feature Selection	107
4.4.1	Feature Extraction	108
4.4.2	Feature Reduction	111
4.5	Classification Performance	113
4.6	Processing time	116

## **CHAPTER FIVE: CONCLUSION AND FUTURE WORKS**

5.1	Introduction	118
5.2	Conclusion	118
5.3	Recommendation for Future Study	121

<b>REFERENCES</b>		123
-------------------	--	-----

## **APPENDICES**

Appendix A:	Example of Radon transform.
Appendix B:	The formulation of support vector machine (SVM).
Appendix C:	Example of Twin Bounded SVM.
Appendix D:	The comparison result of variant ADFs (a) ground truth, (b) (Perona and Malik, 1990), (c) (Tsai <i>et al.</i> , 2010), (d) (Anwar and Abdullah, 2014), and (e) improved ADF algorithms.
Appendix E:	The effect of varying parameter $K$ on FOM calculated from Perona and Malik (1990) and Tsai <i>et al.</i> (2010) algorithms.
Appendix F	The comparison result of thresholding methods (a) ground truth, (b) Otsu's thresholding, (c) Sobel edge detector, (d) Canny edge detector, and (e) proposed double thresholding technique.

## LIST OF TABLES

		Page
Table 2.1	A summary of anisotropic diffusion filter.	20
Table 2.2	A summary of segmentation techniques.	29
Table 2.3	A summary of shape descriptor techniques.	35
Table 3.1	The number of egg samples for training and testing.	75
Table 4.1	Edge evaluation performance.	101
Table 4.2	The comparison of thresholding methods performance.	107
Table 4.3	The performance of TBSVM compared to the standard SVM.	114
Table 4.4	The processing time for crack detection	116

## LIST OF FIGURES

		Page
Figure 1.1	An example of enhanced crack pixels after implementing background illumination strategy.	7
Figure 2.1	An example of bimodal and unimodal histograms.	24
Figure 2.2	An example of projection of $y$ -axis and $x$ -axis of a simple function.	37
Figure 2.3	Radon transform mapping process.	39
Figure 2.4	An example of (a) single hyperplane of SVM and (b) two non-parallel hyperplanes of TBSVM. In this case $\circ$ corresponds to positive class and $\diamond$ corresponds to negative class.	42
Figure 2.5	An example of DAG approach for 3-class classification. The numbers 1, 2 and 3 in the graph denotes intact, micro-crack and macro-crack class respectively. Abbreviations “vs” stands for versus.	47
Figure 3.1	A kernel for line enhancement.	58
Figure 3.2	Crack analysis showing (a) an example of micro-crack and macro-crack samples (b) close-up region views of micro-crack and macro-crack pixels (c) scan line profiles plotted along dotted lines in (b), and (d) gradient profiles of (c). Here, (i) and (ii) correspond to micro-crack and macro-crack samples.	59
Figure 3.3	Laplacian neighbours of pixel $(x, y)$ .	61
Figure 3.4	The effect of varying $s$ on $c(s)$ comparing Equation (3.7) (Perona and Malik (1990)), Equation (2.2) (Anwar and Abdullah (2014)) and Equation (3.8) (improved ADF in this work).	65
Figure 3.5	The effect of varying $s$ and $g$ on $c(s)$ .	66
Figure 3.6	Structuring element of $3 \times 3$ .	70
Figure 3.7	Hardware set-up for crack detection.	73
Figure 3.8	The procedures of image capturing process.	74
Figure 3.9	Example of eggshell image captured (a) without candling light, and (b) with candling light where (i), (ii) and (iii) correspond to	75



intact, micro-crack and macro-crack samples. The dotted circles in (b)(ii) and (b)(iii) show the locations of micro-crack and macro-crack pixels.

Figure 3.10	Block diagram of image segmentation steps.	78
Figure 3.11	Example of matrix $Y$	80
Figure 3.12	Confusion matrix of intact class where 1 (intact), 2 (micro-crack) and 3 (macro-crack). (a) the characteristic fractions with respect to intact class, (b) the sensitivity, (c) the specificity and (d) the accuracy.	84
Figure 3.13	Confusion matrix of micro-crack class where 1 (intact), 2 (micro-crack) and 3 (macro-crack). (a) the characteristic fractions with respect to micro-crack class, (b) the sensitivity, (c) the specificity and (d) the accuracy.	84
Figure 3.14	Confusion matrix of macro-crack class where 1 (intact), 2 (micro-crack) and 3 (macro-crack). (a) the characteristic fractions with respect to macro-crack class, (b) the sensitivity, (c) the specificity and (d) the accuracy.	85
Figure 3.15	The type of ROC performance corresponding to (a) good separation, (b) reasonable, (c) poor separation, and (d) random separation.	86
Figure 3.16	Block diagram of cracks detection system	88
Figure 4.1	Example of texture defects on eggshell surface marked in dotted circles corresponds to (a) dirt, (b) stains, (c) scratches and (d) white-spot respectively. The solid circle in (d) show the location of micro-crack.	90
Figure 4.2	$RGB$ images of Figure 3.9(b) visualized in (a) $R$ channel, (b) $G$ channel, and (c) $B$ channel. Here (i), (ii), (iii) correspond to intact, micro-crack and macro-crack samples respectively.	91
Figure 4.3	Histogram of $R$ , $G$ and $B$ channels corresponding to Figure 4.2. (a) intact, (b) micro-crack, and (c) macro-crack samples.	92
Figure 4.4	Results after background subtraction of images in Figure 4.2(a). Here (a), (b) and (c) correspond to intact, micro-crack and macro-crack samples respectively.	94
Figure 4.5	The performance of line enhancement of different step sizes.	95

Figure 4.6	Results after line enhancement of Figure 4.4. In this case (a), (b) and (c) correspond to intact, micro-crack and macro-crack samples respectively.	95
Figure 4.7	Intensity of crack pixels. (a) and (b) close-up view of micro-crack and macro-crack pixels, (c) and (d) profiles along dotted lines corresponding to figures (a) and (b). Here (i) before line enhancement (ii) after line enhancement.	96
Figure 4.8	The result of image filtering using anisotropic diffusion filter. (i), (ii) and (iii) denote the intact, micro-crack and macro-crack samples respectively. In this case, (a) is a filtered image with iteration $t = 0$ , (b) is an enhanced image with iteration $t = 10$ , $b_r = 0.05$ and $\epsilon = 128$ , and (c) is a subtracted image.	97
Figure 4.9	The effect of different iteration numbers based on FOM measure.	99
Figure 4.10	Results after double thresholding of Figure 4.8(c). Here (a) seed images, (b) target images, (c) reconstructed images, and (d) images after morphological smoothing. In this case (i) intact, (ii) micro-crack, and (iii) macro-crack samples.	103
Figure 4.11	Image after intensity tracing of Figure 4.10(d).	104
Figure 4.12	The results comparing line quality before and after intensity tracing in terms of FOM measure.	105
Figure 4.13	Results from Radon transformation of Figure 4.11, (a) intact, (b) micro-crack, and (c) macro-crack samples.	110
Figure 4.14	Concentricity measures comparing intact, micro-crack and macro-crack samples.	110
Figure 4.15	Results of the sorted features of Figure 4.14 corresponding to intact, micro-crack and macro-crack samples.	111
Figure 4.16	Discriminant separations produced by Wilks' lambda method	113
Figure 4.17	ROC of intact versus macro-crack groups, comparing (a) TBSVM and (b) SVM performance.	115
Figure 4.18	ROC of intact versus micro-crack groups, comparing (a) TBSVM and (b) SVM performance.	115
Figure 4.19	ROC of micro-crack versus macro-crack groups, comparing (a) TBSVM and (b) SVM performance.	116

## LIST OF ABBREVIATIONS

1-D	One-Dimensional
2-D	Two-Dimensional
ADF	Anisotropic Diffusion Filter
AR	Acoustic Response
AUC	Area Under Curve
B	Blue Channel
CV	Computer Vision
DAG	Directed Acyclic Graph
DFT	Discrete Fourier Transform
FD	Fourier Descriptor
FN	False Negative
FOM	Figure of Merit
FP	False Positive
FT	Fourier Transform
G	Green Channel
GFD	Generic Fourier Descriptor
MAD	Medium Absolute Deviation
NN	Neural Network
OVA	One Versus All
OVO	One Versus One
PDE	Partial Differential Equation
QP	Quadratic Programming
R	Red Channel
RBF	Radial Basis Function
RDF	Restricted Dissimilarity Function
RGB	Red Green Blue
ROC	Receiver Operating Characteristic
RST	Rotation, Scaling and Translation
RT	Radon Transform
SNR	Signal to Noise Ratio

SVM	Support Vector Machine
TBSVM	Twin Bounded Support Vector Machine
TN	True Negative
TP	True Positive
WD	Wavelet Descriptor
WT	Wavelet Transform

## LIST OF SYMBOLS

$b$	Bias
$b_r$	Gradient of the sigmoidal ramp
$c$	Diffusion coefficient
$f$	Decision function
$g$	Sigmoid transfer function
$k$	User defined parameter
$m \times n$	Projection matrix of Radon transform
$r$	Distance
$r, \theta$	Radon space coordinate
$s$	Gradient magnitude
$t$	Iteration
$w$	Weight vector
$x, y$	Spatial domain coordinate
$y$	Data label
$C, C_1, C_2, C_3, C_4$	Penalty parameters
$I$	Image
$K$	Edge stopping threshold
$N$	Number of classes
$X$	Concentricity measure
$X_s$	Sorted features
$\vec{X}$	Reduced features
$Y$	Accumulator array
$\alpha_s, \alpha_t$	Scaling factors
$\alpha, \alpha_L, \gamma_L$	Lagrangian multiplier
$\epsilon$	Sigmoidal centre mapping
$\gamma$	Standard deviation
$\mu$	Mean
$l$	Number of element
$\tau$	Threshold
$\nabla$	Gradient

$\zeta, \xi, \eta$	Slack variables
$\tilde{\gamma}$	Gamma
$\theta$	Angle
$-$	Negative
$+$	Positive
$\mathcal{K}$	Kernel
$\mathcal{R}$	Real number
$T$	Transpose
$\phi$	Non-linear map
$\langle \cdot \rangle$	Inner product
$\text{div}$	Divergent operator
$\  \cdot \ $	Norm
$\max$	Maximize
$\min$	Minimize
$\text{s. t}$	Subject to
$\text{sign}$	Sign

# **PENGESANAN RETAK PADA KULIT TELUR MELALUI PENAPIS TAK-ISOTROPI RESAPAN YANG DIPERBAIKI DAN MESIN SOKONGAN VEKTOR**

## **ABSTRAK**

Retak pada kulit telur dikategorikan kepada dua jenis: (i) retak besar, dan (ii) retak halus. Berbeza dengan retak besar, pengesanan retak halus amat sukar dan mencabar kerana kerosakan ini tidak dapat dilihat oleh mata kasar. Sebahagian masalah ini telah diselesaikan menggunakan cahaya “candling” yang direkabentuk khas dengan pemasangan pencahayaan latar belakang. Walaupun penglihatan piksel retak halus telah dipertingkatkan, namun teknik pengimejan ini telah juga meningkatkan struktur-struktur ganjil dan piksel tidak dikehendaki, seterusnya menjadikan imej berselerak dan berhingar. Kaedah tiga peringkat bebas-tingkap dicadangkan untuk menyelesaikan masalah ini. Pada peringkat pertama, penambahbaikan garisan dilaksanakan untuk meningkatkan kualiti garisan di dalam imej. Seterusnya, retak ditambah baik menggunakan penapis tak-isotropi resapan yang diperbaiki. Di dalam kes ini retak ditakrifkan sebagai piksel-piksel yang mempunyai nilai keamatan dan kecerunan yang tinggi. Menggunakan takrifan ini, satu kerangka telah dicadangkan untuk mengesan kulit telur dan mengklasifikasikannya kepada salah satu daripada tiga kemungkinan berikut: (i) utuh, (ii) retak halus, dan (iii) retak besar. Pada peringkat ketiga, kaedah dwi pengambangan yang diubah suai digunakan untuk menambah baik lagi piksel-piksel yang retak. Keputusan menunjukkan kaedah yang diperbaiki adalah berdaya saing apabila dibandingkan dengan teknik-teknik sedia ada dan prestasi lebih baik dicapai dari segi FOM. Secara purata kaedah diperbaiki menghasilkan FOM sebanyak 0.73 berbanding dengan 0.67, 0.57 dan 0.42 yang dihasilkan oleh penapis tak isotropi

resapan yang asal dan dua jenis penapis tak-isotropi resapan yang terkini untuk penambahbaikan retak dan FOM 0.52, 0.68 dan 0.48 yang dihasilkan oleh teknik Otsu, Sobel dan Canny bagi segmentasi imej masing-masingnya. Sementara itu, klasifikasi telah dilaksanakan menggunakan kaedah yang terkini iaitu mesin sokongan vektor kembar terbatas dan keputusan telah dibandingkan dengan kaedah mesin sokongan vektor yang standard menggunakan tiga pendekatan berbeza, iaitu (i) satu-lawan-semua, (ii) satu-lawan-satu, dan (iii) graf asiklik terarah. Keputusan menunjukkan graf asiklik terarah jauh lebih unggul daripada satu-lawan-semua dan satu-lawan-satu dengan purata kepekaan, kekhususan dan ketepatan 93.1%, 96.5% dan 93.0% untuk mesin sokongan vektor kembar terbatas berbanding dengan 90.7%, 95.4% dan 90.7% bagi kaedah mesin sokongan vektor yang standard. Sementara itu, prestasi ROC menunjukkan pengelas dapat membezakan antara sampel utuh dan sampel retak besar dengan 100% ketepatan. Prestasi berkurang tetapi tidak ketara apabila membezakan sampel utuh daripada sampel retak halus dan juga sampel retak halus daripada sampel retak besar. Oleh itu, keputusan ini menunjukkan sistem pengesanan yang dicadangkan adalah berguna dan berkesan untuk aplikasi dalam pemrosesan telur.



# **CRACK DETECTION OF EGGSHELL FEATURING AN IMPROVED ANISOTROPIC DIFFUSION FILTER AND SUPPORT VECTOR MACHINE**

## **ABSTRACT**

Cracks on eggshell are categorized into two types: (i) macro-crack, and (ii) micro-crack. Unlike macro-crack, the detection of micro-crack is very difficult and challenging since this type of defect is invisible to naked eyes. This problem has been partially solved by utilizing a custom made candling light in the background illumination set-up. Even though this has improved the visibility of micro-crack pixels, however this imaging technique has also enhanced anomalies and other unwanted pixels, leading to a very cluttered and noisy images. A three-stage window-free method was proposed to solve this problem. In the first stage, line enhancement was implemented in order to enhance the quality of line in the image. Next, the crack enhancement was performed using an improved anisotropic diffusion filter. In this case, cracks are characterized by pixels having high intensity and high gradient values. Using these characteristics, the detection system has been developed to inspect eggshells and classify them into one of the following three possible classes: (i) intact, (ii) micro-crack, and (iii) macro-crack. In the third stage, a modified double thresholding was employed to further highlight crack pixels. Results indicate that the proposed method is competitive when compared with existing techniques and achieved better performance in terms of FOM. On average the method has resulted in FOM of 0.73 compared to 0.67, 0.57 and 0.42 produced by the original and two recent variants of anisotropic diffusion filter for crack enhancement, and 0.52, 0.68 and 0.48 produced by Otsu, Sobel and Canny techniques for image segmentation. Meanwhile the classifications has been performed using the state of the art twin bounded support

vector machine (TBSVM) and the results have been compared with the standard support vector machine (SVM) utilizing three different approaches: (i) one-versus-all (OVA), (ii) one-versus-one (OVO), and (iii) directed acyclic graph (DAG). Results reveal that DAG outperforms OVA and OVO with sensitivity, specificity and accuracy averaging at 93.1%, 96.5% and 93.0% for TBSVM compared to 90.7%, 95.4% and 90.7% for standard SVM. Meanwhile the ROC performance indicates that this classifier can distinguish between intact and macro-crack samples with 100% certainty. The performance decreases insignificantly when distinguishing intact from micro-crack and micro-crack from macro-crack samples. Therefore, these results suggest that the proposed detection system is useful and effective for applications in egg processing.

# CHAPTER ONE

## INTRODUCTION

### 1.1 Introduction

This chapter presents a brief introduction of egg processing in the poultry manufacturing industry and some of the difficulties and challenges faced by operators during the grading process. The problems and objectives in this research study together with the research scope are also presented.

### 1.2 Crack inspection

Currently, the rate of processing eggs is commonly up to 120,000 eggs per hour in the poultry manufacturing production (Lawrence *et al.*, 2008). The rise in the number of eggs processed per hour consequently requires an increase in the speed of the machine. However, the quality of the eggs must be properly preserved during the process to ensure that the integrity of the eggs remain unchanged for the egg sorting (Yongyu *et al.*, 2012). The determination of the quality of eggs is a very important inspection process in the poultry farming to meet the customers' demand and for food hygiene. Generally, two aspects are scrutinized during the inspection process i.e. (i) internal and (ii) external qualities. Internal quality refers to the egg content such as freshness, blood spot, meat spot and albumen thickness. While external quality refers to the condition of the eggshell such as presence of dirt, stains and cracks. At the external quality inspection, the eggshell is particularly scrutinized for cracks before proceeding to the packaging or sorting stages.

Based on the standards set by European Union Marketing Regulation (European Commission, 2003), eggshells with any external defect such as dirt, stains and cracks will not be permitted to be distributed for marketing purposes. Hence,

quality inspection is an essential process to ensure the poultry marketing meets the standard requirement set by the egg quality regulations. In the grading stage, eggs are sorted according to its quality namely, (i) good or intact and (ii) defect samples. The grading handling is an essential process to sort egg samples before distribution to stores for consumption. In the egg trade, the consumer's first impression is always based on their perception of the shell quality. Any sign of a broken shell would lower the quality of an egg, making it less saleable. A broken egg can also cause the egg content to exude through the cracks in the shell, thus increasing the risk of bacterial infection and food safety (Xiaoyan *et al.*, 2010). A number of studies show that cracked eggs may be exposed to bacteria such as *Salmonella Enteritidis* and *Campylobacter Jejuni* that can infect the egg (Anita *et al.*, 1989), (Ernst *et al.*, 1998), (Hara-Kudo *et al.*, 2001). Hence, shell quality inspection is very important to reduce such risks to human health.

According to the Standard Research Institute of Malaysia (SIRIM) (MS 680:2013., 2013), egg grading sorting is classified into two types: (i) broken and (ii) unbroken samples. In many cases an unbroken egg is referred to as an intact or good egg and a broken egg is referred to as a cracked egg. Meanwhile eggshell crack is categorized into two types: (i) macro-crack and (ii) micro-crack. A macro-crack is a large crack which can be seen by the naked eye like the gross and star cracks while a micro-crack is a hairline crack which is more difficult to see by the naked eye (Bain *et al.*, 2006).

To-date in Malaysia, the egg handling operations such as cleaning and packaging are already automated (Eggtech Manufacturing Sdn. Bhd., (2000), Heap Soon Farming Sdn. Bhd., (2006)). However crack inspections are still done manually or semi-manually. Generally, the inspection is performed by trained operators who look out for any sign of cracks on the shell by viewing the egg from different angles.

Therefore this process is subjective due to the variability of operators and is a very time consuming and tedious process. Be that as it may, this process is still used for crack inspections due to the absence of techniques which are expeditious and accurate for the detection process.

Consequently, developing an automated inspection system in the grading process especially in sorting the good and defect samples is crucial. Replacing the manual and semi-manual inspections which are now performed by trained operators with an automated inspection would reduce the cost of operations and satisfy the customers' demands in terms of egg quality (Mansoori *et al.*, 2011). Besides, the introduction of an automated system for crack detection could particularly minimize the error of detecting micro-cracks. With the width of a micro-crack and macro-crack ranging from 0.02 to 0.04 mm (Orlova *et al.*, 2012) and 0.06 to 1.13 mm (Sun *et al.*, 2018) respectively, the detection of micro-crack is more difficult than macro-crack because this type of defect can only be visualized electronically. Meanwhile, the average crack length is approximately 3.39 cm for both cases (Khabisi *et al.*, 2012). In spite of this difficulty, however, several attempts have been made to develop an automated crack detection system. To-date two techniques are used for crack detection in eggshells which are, (i) acoustic response (AR) (Cho *et al.*, 2000), (Wang and Jiang, 2005) and (ii) computer vision (CV) (Lawrence *et al.*, 2008), (Pourreza *et al.*, 2008). Although the AR method is more popular than CV, the AR detection process is much slower than the CV method because of the hardware set-up involved in the detection process. Although the CV detection is much faster, the detection accuracy is lower compared to the AR particularly in detecting micro-cracks due to the difficulty in recognizing these type of cracks. In the CV inspection, a lighting source is used to enhance cracks. However in most cases, other textures may also appear during the inspection which can complicate the recognition of

cracks. Therefore, there is still work which needs to be done in the CV inspection in order to overcome this problem.

### **1.3 Research problems**

As discussed in the previous section, two approaches are used to detect cracks namely the AR (Cho *et al.*, 2000), (Wang and Jiang, 2005) and CV (Lawrence *et al.*, 2008), (Pourreza *et al.*, 2008). Both approaches use different inspection measurements. In summary, the AR is based on the measurement of the frequency response produced by inflicting a light mechanical impact at various angles onto the surface of the eggshell equator. This is very time consuming processing and also requires calibration and fine adjustment of hardware. On the other hand, the CV measurement uses candling light as a source of illumination which enables both the exterior and interior properties of an egg to be visualized. Also, the machine set-up for CV is not too complicated compared to the AR system as the CV capturing process only requires the eggs to be placed on top of the illumination source and adjusting the focal length of a camera. The micro-crack forms white pixels in the image since the shell membranes and fibers are fairly transparent to visible light radiation. A previous study demonstrates the usefulness of this technique in detecting micro-cracks with an accuracy of above 90% (Lawrence *et al.*, 2008), (Yongyu *et al.*, 2012), (Pan *et al.*, 2007). However, these authors performed measurement by force opening the micro-crack using a small vacuum chamber so that this defect can be detected by the CV inspection. In this measurement, a negative pressure of approximately -20 kPa is normally employed to open crack regions so that they can be imaged by cameras (Lawrence *et al.*, 2008). This could irreversibly increase the size of a crack, resulting in a permanent damage to a shell if excessive pressure is applied. Therefore it is generally preferred for the inspection to be performed at

atmospheric pressure as reported in the work by Pan *et al.* (2011), however the detection rate obtained from this study is relatively low, averaging slightly over 60% especially when inspecting micro-crack samples. Lower detection accuracy was the results of the deployment of simple and standard image processing algorithm. In this case, these authors used median filter to reduce noise which also blurred the important edges of crack. Similarly single threshold value that was used to segment between crack and unwanted pixels was not suitable for images whose intensity values vary from one pixel to another as in eggshell image. Also the accuracy of the CV method depends critically on the types of eggshell cuticles, the intensity of which varies from one egg to another. Therefore the use of simple thresholding technique would result in large number of eggs been misclassified as evident from the work by Pan *et al.* (2011).

Chemically, the cuticle comprises of 85-90% proteins, polysaccharides 4%, lipids 3% and porphyrin pigments, and this composition depends on various factors such as the freshness, hen age and genetics (Rodríguez-Navarro *et al.*, 2013). These materials are responsible for the complicated heterogeneous textures of the eggshell especially when viewed under the candling light. The presence of other anomalies such as dirt, scratches and grains can increase the complexity of the CV images making the process of crack detection more difficult. Therefore, the CV detection system requires a very reliable algorithm to process the captured image to reduce false detection during inspection. One of the techniques that is increasingly being used in the application of crack detection is anisotropic diffusion filter (ADF). The advantage of this filtering technique is the detail of edges is well preserved whilst smoothing other unwanted pixels. This filtering is useful in enhancing crack pixels in the image that containing unwanted components such as dirt, scratches and grains. Besides the convolution process of this filtering produces equal response to any

pixels in the image that including crack pixels compared to a simple edge detector which tend to produce two lines in the image resulting in many false edges detection. An improvement on the original ADF can still be made especially in determining the edge stopping threshold as the original ADF uses a singular value. This singular value is not suitable for the curvature shape object like an egg because the image when view under camera would be non-uniformly illuminated. Besides this value is determined using trial-and-error approach. In this case, higher value will significantly diffuse the image resulting in image blurring while lower value will terminate the diffusion process causing no significant change in the output image. Many attempts have been made in determining the edge stopping threshold value. One of the latest attempts was proposed by Anwar and Abdullah, (2014). In this work, a singular value used in the original ADF has been replaced with dynamic values calculated using the sigmoid transfer function by utilizing the intensity values of the input image. This proposed method is suitable for the case of uneven illumination image. However this ADF variant is very effective when the diffusion is intended for pixels having low gray scale values but high gradients. Therefore this method is only suitable for selected application especially in the electroluminescence imaging which was investigated by these authors. Clearly this method needs to be further developed in order to enhance crack pixels in images acquired using different imaging technology like the candling light illumination.

In addition to the difficulties and problems in detecting micro-crack pixels as mentioned earlier, in some cases the similarity between a micro-crack and other texture pixels is an added challenge in this study as depicted in Figure 1.1. This similarity complicates the detection of the micro-crack pixels because of the possibility that the micro-crack sample is detected as an intact sample and vice-versa. This problem presents a challenge for micro-crack detection using the CV approach.



Therefore, the implementation of image processing and machine learning techniques is crucial to minimize the misclassification detection between class samples during the inspection process. These problems led to the objectives in this study as mentioned in the following section.

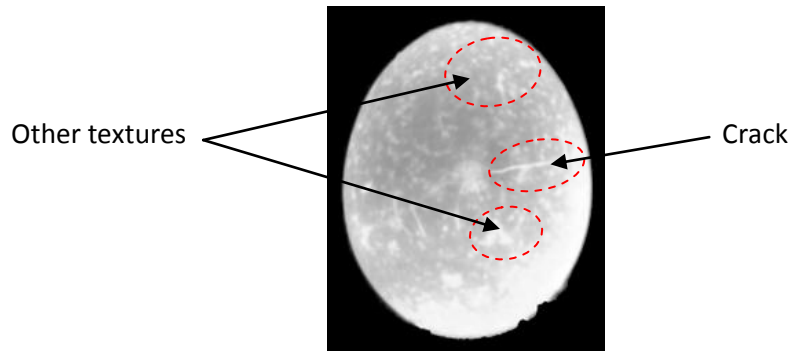


Figure 1.1: An example of enhanced crack pixels after implementing background illumination strategy (Sun *et al.*, 2018).

#### 1.4 Research objectives

In this study, a crack detection system using the computer vision approach was investigated. This detection integrates the image processing and machine learning platform to solve the problems of crack inspection in poultry processing. Hence, the following objectives were set:

1. To set-up a machine vision hardware to visualize cracks on eggshell.
2. To develop an image processing algorithm for crack enhancement.
3. To investigate image segmentation technique for highlighting crack pixels in the image.
4. To classify cracks into different defect categories.

These objectives serve as a guideline for the overall research procedures in this work.

## **1.5 Research scope**

The detection of crack on eggshell during the egg grading is important to maintain the quality of egg before it reaches to consumers. However the use of existing automated computer vision approach in detecting crack especially micro-crack still produces a low detection in accuracy. In the presence of other unwanted structures in the image, the detection becomes more complicated. Hence the scope area of this research is to study the use of image processing technique and machine learning in solving the problems of crack detection in the computer vision approach. Here, only the fresh laid chicken eggs produced by local farmers are considered. The outcome of this research study is important to ensure the quality of egg is maintained and in the end it could benefit the human health.

## **1.6 Thesis organization**

A brief explanation of the whole work in this study is expressed in this section to facilitate the understanding of the objectives and procedures used in this research. The second chapter presents the literature review of previous studies on crack detection. Next, Chapter 3 discusses the theory of proposed methods used in this work. Also, it discusses the methodology used in the detection procedures namely image processing, segmentation technique, feature extraction and classification. The results of the experimental works starting from the image capturing until the classification process together with the results of detection and classification accuracy is presented in Chapter 4. Chapter 5 concludes the findings of this research and future works.

## **CHAPTER TWO**

### **LITERATURE REVIEW**

#### **2.1 Introduction**

This chapter reviews significant points of existing and prior studies on crack detection comprising the knowledge, findings, theories and methodology. Also, this chapter covers three important aspects namely image processing, pattern representation and machine learning in developing the system. In the first aspect, two main areas are discussed in the image processing (i) image pre-processing and (ii) segmentation process. The image pre-processing highlights the importance of using filtering techniques to enhance the targeted pixel in the image while the segmentation process emphasizes on the selected thresholding method to segment the targeted objects. The second aspect describes the importance of pattern representation in representing the objects for further processing. Meanwhile, machine learning emphasizes on the classification method in classifying samples into proper classes. Also, this chapter presents the results and methods on eggshell crack and other crack detection application from works previously done by other researchers. The findings of these review works were highlighted in the summary section at the end of this chapter which lead to the proposed detection system in this study.

#### **2.2 Image processing**

In the evaluation of computer vision applications, image processing is the most important part in solving vision problems (Malamas *et al.*, 2003). Theoretically in an image processing application, the degree of difficulty in solving the processing method increases with the complexity of the image information. Two stages are involved in the image processing (i) pre-processing and (ii) segmentation (Sonka *et al.*, 2008). The approaches involved in implementing these stages are different. In the

pre-processing stage, many techniques can be applied depending entirely on the application involved such as enhancement, denoising, edge detection, compression and restoration and the techniques in this stage can be implemented and processed in the spatial domain. Whereas in the image segmentation stage, the process of detection is carried out to segregate the targeted objects and remove the unwanted objects by implementing thresholding techniques (Gonzalez & Woods, 2002).

### **2.3 Anisotropic diffusion filter**

Generally, image filtering and edge detection are the common processes engaged in an image pre-processing process. The aim of implementing pre-processing is to suppress the unwanted distortions and enhance the important pixels of the structure for further analysis. There are two popular methods used in the image pre-processing process: (i) spatial domain and (ii) frequency domain. In the spatial domain method, an image is processed by convolving it with the filter mask where the selection of filter mask depends on the application. The process involved in frequency domain differs from the spatial domain filtering in that in frequency domain filtering, an image is first transformed into frequency domain by implementing discrete Fourier Transform (DFT). Instead of using the convolution process in the filtering process as in spatial domain, the frequency domain uses a multiplication process in filtering the spectrum with the filter function (Gonzalez & Woods, 2002), after which the filtered image can be visualized by using the inverse transformation process.

In image pre-processing, the most important part is to preserve or enhance the information on the edges since it contains ample amount of image description so that it can be used in further analysis. The superior edge detection technique will be considered precise if it is able to detect and localize edges and hold the edges representation accurately (Yupeng & Jiangyun, 2016). The edges are computed by

convolving the image with a gradient operator known as mask with a normal size of  $3 \times 3$  pixels. The derivatives of the image are obtained by applying a gradient operator to estimate the differences in the gray value with neighboring pixels (Sonka *et al.*, 2008). In examining edges directions, the convolution process may sometimes need to be executed more than once where a gradient operator has a number of masks to be convolved. At every convolution process, the edges are constructed by computing the magnitude response. For instance, the Sobel gradient operator calculates the changes of two directions namely vertical and horizontal and performs the convolution process for both directions in the image.

While the filtering process has effectively reduced noises and smoothen the image, it has also resulted in the blurring of the edges. There is a filtering technique called anisotropic diffusion filter which can reduce the image noise while preserving the edges (Perona & Malik, 1990). The approach used in this filtering technique resembles the scheme of scale-space filtering where it iteratively convolves the image with the filter of variable scales (Witkin, 1984). However, the smoothing effect in anisotropic diffusion is formed by a process of diffusion resulting in a blurred image depending on the local content of the original image. The diffusion process is performed by convolving the original image with a nonlinear filter with certain iteration (Perona & Malik, 1990). Mathematically it is given as follows:

$$\frac{\partial}{\partial t} I(x, y, t) = \text{div}(c(|\nabla I|)\nabla I) \quad (2.1)$$

where  $t$ ,  $c$  and  $\nabla$  are iteration, the diffusion coefficient and gradient respectively. The  $\text{div}$  is a divergence operator. The diffusion coefficient  $c$  controls the rate of diffusion and is chosen as a function of gradient magnitude  $|\nabla I|$  to preserve the image edges. In this case, the gradient magnitude is obtained by computing all four nearest neighboring pixels in every direction similar to a Laplacian operator. The diffusion

coefficient is a nonnegative value which varies from 0 to 1 and has a monotonically decreasing function with respect to the gradient magnitude. In this case, higher values of diffusion coefficient will affect the smaller gradient magnitude and produce a smoothing effect on the particular pixels while locations with higher gradient magnitude are less diffused and will preserve the preferred structure of higher pixels especially the edges. Principally, any pixel with a gradient magnitude less than the edge stopping threshold will be smoothen during the filtering process. However, the rate of a diffusion model in Equation (2.1) to filter the noise and preserve the edge details depends on the value of edge stopping threshold. In most cases, the edge stopping threshold is manually fixed through a trial-and-error experiment. This is the main drawback of Perona and Malik's equation.

To date a number of studies have been done after the anisotropic diffusion filter was proposed by Perona and Malik (1990). Earlier studies were carried out to understand the structure of anisotropic diffusion on its mathematical formulation and properties plus its application on image processing such as edges detection, enhancement, segmentation and noise reduction. Thereafter a further study on the standard diffusion model and coefficients discovered that it could produce a diverging solution to the image with a high similarity (Catté *et al.*, 1992). This problem is solved by convolving the gradient of the image with a low pass filter prior to the execution of the diffusion process. Furthermore, extension and modification on anisotropic diffusion equation were made to create a fast and accurate system to suit its application (Gerig *et al.*, 1992).

The statistical interpretation of anisotropic diffusion and robust statistics was examined and the results demonstrated an improvement in relation to these two models (Black *et al.*, 1998). The improvement in a robust statistic demonstrated that the use of a medium absolute deviation (MAD) to estimate the edge stopping

threshold has improved the diffusion process where the preservation of edges in the output image improved greatly. Meanwhile Acton (1998) implemented a multi-grid technique in anisotropic diffusion for image enhancement. This strategy resulted in a lower computational cost of diffusion process and the elimination of low frequency noises in the output image. Further improvement was investigated using the variation of edge stopping threshold by utilizing the diffusion coefficient (Monteil & Beghdadi, 1999). In this work, substantial noise could be eliminated as the transition gradient range was well preserved compared to the conventional anisotropic diffusion approach. For this approach it was assumed that some parts of the images were texturally identical and the distribution of noise was equal in most areas in generating the edge stopping threshold.

In the work proposed by Weickert (1999), the approach known as second moment matrix (structure tensor) in enhancing the image with a flow-like pattern was used. In this case, they used the cohesion direction of pixels contrast to calculate the diffusion coefficient and the results revealed that the use of structure tensor technique is suited for solving the problem of flow-like patterns image. In addition, the same approach was investigated in the work of Deguchi *et al.* (2002) by utilizing the structural analysis tensor in detecting and enhancing the line structures in a gray-level image. In this work, anisotropic diffusion filter was incorporated into the multi-resolution image analysis as the results demonstrated that the line structures have been enhanced.

A further study on diffusion process was carried out to enhance edges as proposed by Gilboa *et al.* (2002). In this work, the concept of forward and backward (FAB) adaptive filtering was utilized in enhancing the features (backward process) while locally smoothing segments of the images (forward process). Even though the enhancement scheme showing the image quality produced better results, the FAB

approach is not suitable for processing of images with high textures and high gradient bands. In another approach, a combination of modified anisotropic diffusion filter and a scale-based image enhancement method was investigated by Song and Choi (2004). In this work, the diffusion process was calculated by using the local gradient and the critical value function which was obtained by modifying the standard anisotropic diffusion to estimate noise. Using the relationship between local gradient and the function, the image was divided into various scales of region where the enhancement process for each region were tuned based on the complexity of the image. The results indicated that the proposed method produced an image with significantly less noise and well preserved edge details.

A further study on anisotropic diffusion model was carried out in image segmentation by Voci *et al.* (2004). In this work the regularized model of anisotropic diffusion was proposed to segment the image and reduce the noise by using scale-space analysis. Also, this work proposed two different methods in calculating an automatic edge stopping threshold using the approach of morphological and the simple calculation of  $p$ -norm. The use of Lyapunov function of  $p$ -norm showed a decreasing edge stopping threshold and resulted in the preservation of details due to the lasting diffusion process. Meanwhile, the generalization of fractional-order diffusion model using Euler-Lagrange cost-functional formulation was investigated by Jian and Xiang-Chu (2007) for image denoising. This implementation was performed using the second-order and fourth-order of anisotropic diffusion model. In this analysis, the diffusion process was carried out in the frequency domain and to counter the problem of periodic boundary condition in the input image, a folded algorithm was performed by widening the input image symmetrically about its border. The result demonstrated that the fractional-order approach in this work produced a better image with less noise.



Meanwhile, a modification to anisotropic diffusion model was further studied in the work by Yu *et al.* (2008) by incorporating a kernel method into anisotropic diffusion model to produce an image with less noise and enhanced edges. In this work, the input image was firstly mapped into a feature space and the estimation of diffusion threshold was adaptively calculated in the feature space using the function of the MAD. The results demonstrated that the kernel method incorporated into the anisotropic diffusion outperformed the conventional diffusion method in reducing noises and preserving edges for low signal-to-noise ratio images. In a subsequent attempt, a method called a variation of window sizes was proposed by Liu *et al.* (2009) to estimate the anisotropic diffusion coefficient. In this work, the estimation of diffusion coefficient was determined adaptively based on variation of window size and orientation of the image. Changes in the window size depended on the local image structure and in this case the window size was broadened over the smooth area and minimized over the edges. The outcome of this method demonstrated that the use of dynamic window size to estimate the diffusion coefficient based on local image structure produced a satisfactory result in suppressing speckles and preserving edges compared to the existing methods. However the window direction must be first determined before calculating the diffusion coefficients. In this case the window must be in the rectangular form. The operation of rotation and translation needs to be carried out if the window is not in the rectangular form leading to higher processing time.

A coupled partial differential equation (PDE) was investigated in denoising the multispectral images by incorporating it into anisotropic diffusion (Prasath & Singh, 2010). In this work, the standard anisotropic diffusion was modified to utilize all the inter channel correlation present in the multispectral image. By incorporating a coupled PDE into anisotropic diffusion, the inter channel relations were modeled

which balanced the diffusion process while smoothing the divergence of diffusion process. In this case, the coupling uses weight which is adaptively computed from different bands of input image. The function of weight is to align the edges in the different channels and to stop the diffusion process. The results demonstrated that the multispectral images were well processed by the proposed scheme in removing noises and preserving the detailed features in the image. However the proposed approach was limited to only multispectral images. Further future works should be extended for hyperspectral images. In another work, the combination of subpixel approach and fractional order anisotropic diffusion was proposed for image denoising (Zhang *et al.*, 2011). In this scheme, the Euler-Lagrange equation was used as an increasing function of the fractional derivative of image intensity whilst the subpixel fractional order partial difference was performed in the frequency domain. The results indicated that the scheme managed to overcome the issue of staircasing and blurred effect whilst preserving the important features such as edges, boundary and textures with higher signal-to-noise ratio (SNR). In another approach the second and fourth orders anisotropic diffusion model was investigated in the work by Wang *et al.* (2012) for image denoising. In this study, both models were obtained by using the gradient vector convolution (GVC). In this analysis, the second order was developed by integrating the GVC model into anisotropic diffusion while the fourth order was calculated by incorporating GVC model into the You-Kaveh fourth order model (You & Kaveh, 2000). The advantage of implementing GVC in this scheme is that it can be performed in real time using Fast Fourier Transform (FFT) with less computational cost. The results revealed that the proposed scheme effectively reduced noises while preserving the important edges and textures.

In another application, a generalization of Perona-Malik anisotropic diffusion was studied using a restricted dissimilarity function (RDF) (Lopez-Molina *et al.*,

2013). The function estimates the difference between the intensity values around neighboring pixels. In this analysis, the generalization of Perona-Malik anisotropic diffusion was replaced by the absolute difference between pixels using the RDF. The dissimilarity in RDF is small for the same object but large for the different objects when estimating the intensity of two neighboring pixels where the number of diffusion is determined by this dissimilarity. The flexibility of the RDF analysis incorporated into the anisotropic diffusion was advantageous in estimating the difference between intensity pixels and produced better results. Meanwhile, a gradient-based anisotropic diffusion filtering was examined in the processing of microscopic images (Liu, 2013). In this analysis, the diffusion coefficient was determined by using the attributes of the interior area and boundary area of image. The result indicated that the use of anisotropic diffusion in filtering process produced a promising result compared to the other techniques in preserving the details of the edges and removing the noise in macroscopic images. However this method requires each pixel of the image to be firstly computed to determine whether it belongs to noise or boundary leading to greater computational time.

An improvement on anisotropic diffusion by incorporating weight into the divergence diffusion process was investigated in the work of Prasath and Vorotnikov (2014) for image denoising. The modified scheme incorporated the balance term in the work of Barcelos *et al.* (2003) to offer a well-balanced flow in preserving the details of the edges and removing the noises. The proposed scheme was tested by using noisy images, yielding a good result in detecting the edges and removing the noise. In another attempt, image denoising by means of an anisotropic diffusion-based for image enhancement was inspected by Barbu (2014). The denoising partial differential equation (PDE) approach was derived from the standard Perona-Malik equation. In this scheme, a new diffusivity function serving as edge-stopping was

proposed using a conductance diffusivity where the conductance was computed by using statistical measure. The result of this scheme showed that the developed PDE-based model yields a fine image with less noise with the edges well preserved and enhanced. Recently, an improved modification on anisotropic diffusion model based on new non-local means (NLM) was proposed for image denoising (Yuan, 2015). In this analysis, the incorporation of NLM into anisotropic diffusion process managed to reduce the staircasing effect in the image while preserving details of the edges. The NLM model was generated by estimating the information of intensity, gradient and space position. Besides, the introduction of a gradient term into the anisotropic diffusion produced a better image which can control the smoothing effect. The outcome of this method demonstrated that the proposed scheme has outperformed the existing techniques in reducing noises in the image. In another study, the Perona-Malik anisotropic diffusion function was modified to optimize the Canny operator by replacing the Gaussian filtering process of the conventional Canny operator (Xianhong & Chunrui, 2016). The modified diffusion coefficient function proposed in this work is based upon the analysis conducted on the advantages and disadvantages of two standard diffusion functions of Perona and Malik (1990). The results indicated that the modified operator managed to overcome the limitation of the Gaussian filter (missing edges and false edge detection) and provided protection to the edges as well as removing the noise.

The investigation and implementation of anisotropic diffusion filtering is widely utilized in the application of image processing due to its advantages in the filtering process. In recent years, this filtering approach was used and investigated to enhance defects especially cracks. For instance, anisotropic diffusion filter was applied to process the sensed image of glass substrates containing various textures of defects including cracks (Chao & Tsai, 2008). In this proposal, the smoothing and

sharpening of the image was performed simultaneously with the diffusion process. The result demonstrated that the proposed scheme can perform the detection on low contrast surface. In another application, the detection of micro-crack in the solar wafer using anisotropic diffusion filter was examined by Tsai *et al.* (2010). In this work, the information on both the gray scale and the gradient of the image was investigated in modelling and adjusting the diffusion coefficients. Even though the approach used in this work has capably preserved the detail of edges and reduced the unwanted region, the effectiveness of this analysis is thoroughly based on the selection of edge stopping threshold which is still obtained via trial-and-error experiments. Meanwhile, a new development based on anisotropic diffusion in the work of Chao and Tsai (2008) was further studied by Mhamed *et al.* (2012). This work introduced a new edge stopping threshold technique in detecting crack defects in the radiographic film of pipelines. In this analysis, the edge stopping was modified by incorporating a sharpening function using a sigmoidal function equation. The scheme was tested by using multiple simulations and showed a good performance. In another approach, further development of anisotropic diffusion was investigated in the detection of micro-crack defect in the multicrystalline solar cells (Anwar & Abdullah, 2014). In this scheme, an improved edge stopping threshold was proposed by introducing threshold for each pixel in the image. This threshold is adaptively calculated by mapping the image intensity through the sigmoid transfer function  $g$  using the input image gray value as given in the following equation.

$$c(s) = 1 - 1/[1 + (\frac{s}{g})^2] \quad (2.2)$$

where  $s$ ,  $c(s)$  and  $g$  are the gradient, a diffusion coefficient and the edge stopping threshold. The result demonstrated that the scheme efficiently detected and enhanced the micro-crack region on multicrystalline solar cells and provided a good result in

the segmentation process. Table 2.1 presents the summary of the development of ADF.

Table 2.1: A summary of anisotropic diffusion filter.

Authors	Summary of the methods	Comments
Perona and Malik (1990)	Founders of anisotropic diffusion filter. The proposed method was aimed to reduce noises and preserve edge details.	The main drawback of this method is the edge stopping threshold which needs to be set manually.
Catté <i>et al.</i> (1992)	A slight improvement in the convergence by convolving the gradient image with low pass filter prior to the diffusion process.	Causes image blurring and dislocation of important image features especially edges.
Black <i>et al.</i> (1998)	Introduced a robust statistical measure to estimate edge stopping threshold by manipulating spatial coherence. The results indicated more edges were preserved.	The use of spatial coherence in detecting edges produces a gridlike pattern to the edges that are more than one pixel wide.
Acton (1998)	Implemented multi-grid approach in anisotropic diffusion resulting a lower computational cost. Indirectly the method removed low frequency components.	Edge stopping threshold still needs to be determined through trial-and-error approach.
Monteil and Beghdadi (1999)	A new variant of edge stopping threshold was investigated. The results indicated that large noise were removed from the image.	This approach assumes that some part of the images are texturally homogeneous in generating the edge stopping threshold. Moreover, this method uses a trial-and-error method in choosing the size of homogeneous block to generate edge stopping threshold.
Weickert (1999)	A second moment matrix approach was proposed in solving the flow-like pattern	Principal axis transformation of the

Table 2.1: Continued

	image. In this work, the diffusion coefficients were computed using the cohesion direction of pixels contrast.	structure tensor must be performed for each pixel leading to higher computational time.
Gilboa <i>et al.</i> (2002)	This work used the concept of forward and backward adaptive filtering in smoothing the segment and enhancing the features. A significant improvement in the edge images has been reported.	This approach is not suitable for images with high textures and gradient values.
Song and Choi (2004)	The critical value function was incorporated into a diffusion coefficient by estimating noise in the image based on minimum reliable scale. This method produced good results particularly with inhomogeneous image.	The number of scales used in the analysis must be properly determined to avoid higher computational cost.
Voci <i>et al.</i> (2004)	Two methods in calculating the edge stopping threshold were introduced: (i) the morphological approach and (ii) the simple calculation of $p$ -norm.	The estimation of edge stopping threshold using a morphological approach increases the computational cost.
Jian and Xiang-Chu (2007)	An approach of fractional-order of anisotropic diffusion was proposed in this work. The diffusion process was performed in the frequency domain. The results demonstrated this approach was useful for noise reduction.	Even though the proposed method filtered out most of the noises, however in some cases it produced unwanted staircase or speckle effect.
Yu <i>et al.</i> (2008)	This work incorporated a kernel method into anisotropic diffusion model. The input image was mapped into a feature space then the estimation of diffusion threshold was adaptively calculated in the feature space using the median absolute deviation (MAD). This method was efficient on the image with low signal-to-noise ratio.	A suitable MAD estimator needs to be tested and selected based on various MAD operators for kernel anisotropic diffusion leading to higher processing time.
Liu <i>et al.</i> (2009)	The diffusion coefficient was estimated adaptively using the variation of window size. The method proved to be effective to suppress speckles and preserve edges.	The operation of rotation and translation needs to be carried out if the window is not in the rectangular form leading to higher

Table 2.1: Continued

		processing time.
Tsai <i>et al.</i> (2010)	The information on both the gray scale and the gradient of the image was used in modeling the diffusion coefficients.	The effectiveness of this method depends on the selection of edge stopping threshold which is determined through trial-and-error experiments.
Prasath and Singh (2010)	A couple partial differential equation (PDE) was proposed for denoising the multispectral images. The correlation of inter channel of multispectral images was utilized in developing the diffusion model.	This approach is limited to only multispectral images.
Mhamed <i>et al.</i> (2012)	The edge stopping in the Perona and Malik's equation was modified by incorporating a sharpening function using a sigmoidal function equation yielding a good performance	Sensitive to noise.
Wang <i>et al.</i> (2012)	This work integrated the gradient vector convolution (GVC) into the second and fourth orders anisotropic diffusion. The results indicated that the scheme was effective in reducing noises and preserving edges	Edge stopping threshold is determined using trial-and-error experiment. Also, the denoising ability of fourth order is weak compared to recent diffusion techniques.
Lopez-Molina <i>et al.</i> (2013)	The generalization of Perona-Malik anisotropic diffusion was replaced by the absolute difference between pixels using a restricted dissimilarity function (RDF). The function estimates the difference of intensity values around neighbouring pixels.	The success of a diffusion process relies on the choice of RDF which is image dependent. In this case, undesirable RDF leads to excessive diffusion resulting in removing important edges.
Liu (2013)	In this work, the diffusion coefficient was determined using the interior and boundary areas of an image. This approach produced a good result in preserving the edge details at macroscopic levels.	This method requires each pixel of the image to be firstly computed to determine whether it belongs to noise or boundary. This leads to longer processing



Table 2.1: Continued

		time.
Anwar and Abdullah (2014)	The threshold is calculated by mapping the image intensity through the sigmoid transfer function using the input image.	This method is useful for image having dissimilar pixels between background and foreground.
Barbu (2014)	A new diffusivity model serving as edge-stopping was proposed using a conductance diffusivity resulting a fine image with less noise.	The effectiveness of the model depends on the parameters used for calculating the threshold. These parameters are obtained via trial-and-error approach.
Yuan (2015)	A new non-local means (NLM) was incorporated into anisotropic diffusion. The NLM model was generated by estimating the information of intensity gradient and space position. The method managed to reduce the staircasing effect in the image while preserving details of the edges.	Edge stopping threshold needs to be set manually.
Xianhong and Chunrui (2016)	In this work the Perona-Malik anisotropic diffusion function was modified in order to improve the performance of Canny operator. In this case, the Gaussian filter was replaced with the modified ADF. The method overcomes the limitation of the Gaussian filter.	The use of local approach to determine the threshold leads to an increase of the computational time.

## 2.4 Segmentation

In computer vision, recognizing the targeted objects for further analysis is a tough task to perform as they usually come with other textures. In doing so, image segmentation plays the most important role to distinguish or eliminate the unwanted textures to facilitate the recognition process. The aim of segmentation process is to analyze, divide and represent the region of interest into something that can be recognized by the system. The well-known method that is widely used in the segmentation process is thresholding. In thresholding, the decisive part in

segmenting between the region of interest and background strictly depends on the selection of threshold value. Over the past few years, many works were done to investigate the success of thresholding method in the segmentation application as summarized by Sezgin and Sankur (2004).

In image segmentation, separation between the region of interest and background can be done by using two approaches namely global and local thresholding (Gonzalez & Woods, 2002). For global thresholding, a single or multiple threshold value is used to separate the foreground and background by estimating the histogram of pixel intensity that represents the area of the image. Two methods are used to estimate the threshold value using histogram namely bimodal and unimodal. In the analysis of bimodal, the histogram produces two peaks of intensity which correspond with the region of interest and background. This approach is more suitable in estimating the threshold value of images having a distinct intensity between the region of interest and the background yielding lower overlapping in the plot modality. However, the estimation of threshold value tends to be trickier when the histogram plot produces higher overlappings. Meanwhile, in a case where the pixel intensity is not noticeably distinguishable, then the produced histogram becomes unimodal where distribution usually happens in the image gradient and edge. An example of bimodal and unimodal histograms is depicted in Figure 2.1.

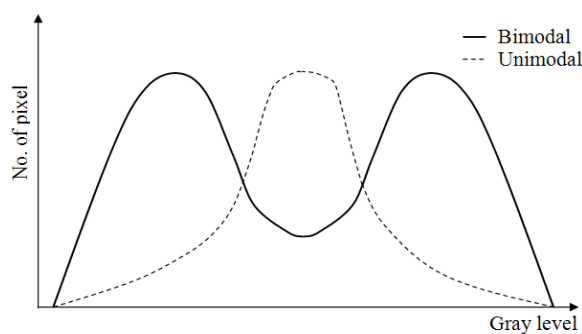


Figure 2.1: An example of bimodal and unimodal histograms.